Current Biology 19, 1730–1735, November 3, 2009 ©2009 Elsevier Ltd All rights reserved DOI 10.1016/j.cub.2009.08.041

Report

Mitochondrial Inheritance Is Required for MEN-Regulated Cytokinesis in Budding Yeast

Luis J. García-Rodríguez,[1,2] David G. Crider,[1,2] Anna Card Gay,[1] Iñigo J. Salanueva,[1] Istvan R. Boldogh,[1] and Liza A. Pon[1,*]
[1]Department of Pathology and Cell Biology, College of Physicians and Surgeons, Columbia University, 630 W. 168th Street, New York, NY 10032, USA

Summary

Mitochondrial inheritance, the transfer of mitochondria from mother to daughter cell during cell division, is essential for daughter cell viability. The mitochore, a mitochondrial protein complex containing Mdm10p, Mdm12p, and Mmm1p, is required for mitochondrial motility leading to inheritance in budding yeast. We observe a defect in cytokinesis in mitochore mutants and another mutant (*mmr1Δ gem1Δ*) with impaired mitochondrial inheritance. This defect is not observed in yeast that have no mitochondrial DNA or defects in mitochondrial protein import or assembly of β-barrel proteins in the mitochondrial outer membrane. Deletion of *MDM10* inhibits contractile-ring closure, but does not inhibit contractile-ring assembly, localization of a chromosomal passenger protein to the spindle during early anaphase, spindle alignment, nucleolar segregation, or nuclear migration during anaphase. Release of the mitotic exit network (MEN) component, Cdc14p, from the nucleolus during anaphase is delayed in *mdm10Δ* cells. Finally, hyperactivation of the MEN by deletion of *BUB2* restores defects in cytokinesis in *mdm10Δ* and *mmr1Δ gem1Δ* cells and reduces the fidelity of mitochondrial segregation between mother and daughter cells in wild-type and *mdm10Δ* cells. Our studies identify a novel MEN-linked regulatory system that inhibits cytokinesis in response to defects in mitochondrial inheritance in budding yeast.

Results and Discussion

Mutations that Inhibit Mitochondrial Inheritance Produce Multibudded Cells in Budding Yeast

Equal segregation of mitochondria between mother and daughter cells during yeast cell division occurs as a result of bidirectional movement of mitochondria to the bud tip and mother cell tip and anchorage of the organelle at those sites [1]. The mitochore, a mitochondrial membrane protein complex containing the proteins Mmm1p, Mdm10p, and Mdm12p, is required for binding of mitochondria to actin filaments in vitro, actin cable-dependent bidirectional mitochondrial movement, and mitochondrial inheritance [1–3]. In early characterizations of mitochondrial morphology and distribution mutants, Sogo and Yaffe [4] noted the presence of a multibudded phenotype in *mdm10Δ* cells. We find that multibudded clusters consisting of 3–5 buds are present during mid-log phase and accumulate with growth time in *mdm10Δ* cells. This multibudded phenotype is observed in *mdm10Δ* cells in three different genetic backgrounds: S288C, W303, and A264A (data not shown).

In wild-type yeast, mitochondria constitute a dynamic and tubular reticulum (Figures 1A and 1B) [1]. In *mdm10Δ* cells, mitochondria are large spherical structures that fail to move from mother cells to buds and undergo rapid loss of mitochondrial DNA (mtDNA) [2, 3]. The large spherical mitochondria typical of *mdm10Δ* cells are usually present in only one cell within a multibudded clump (Figures 1E and 1F). Visualization of DNA confirmed that *mdm10Δ* cells have no mtDNA and revealed that each cell body in *mdm10Δ* clumps contains a nucleus (Figures 1G and 1H). The viability of wild-type and *mdm10Δ* cells during mid-log phase growth, assessed with FUN-1 staining, is 93.5% and 76.5%, respectively. Thus, a mutation in *MDM10* that results in severe defects in mitochondrial morphology and inheritance also produces defects in mother-daughter cell separation but does not inhibit nuclear inheritance or compromise cell viability.

Deletion of *MDM10*, *MDM12*, or *MMM1* also results in defects in maintenance of mtDNA, mitochondrial morphology, and assembly of β-barrel proteins in the mitochondrial outer membrane (OM) [2, 4–6]. Therefore, we tested whether the multibudded phenotype of *mdm10Δ* cells is due to defects in these mitochondrial inheritance-independent processes by analysis of yeast bearing deletions in mtDNA, *MAS37*, or *TOM7*. rho^0 cells have no mtDNA and severe defects in mitochondrial respiration [7]. Mas37p is a subunit of the SAM/TOB complex, which mediates assembly of β-barrel proteins into the mitochondrial OM [8]. Tom7p is a subunit of the protein-translocating pore in the mitochondrial OM [9]. Deletion of *TOM7* produces defects in mitochondrial morphology that are similar to those observed in *mdm10Δ* cells as well as defects in mitochondrial protein import [6]. Tom7p also promotes the segregation of Mdm10p from the SAM/TOB complex [10].

rho^0, *mas37Δ*, and *tom7Δ* cells exhibit significantly lower defects in mitochondrial inheritance and lower levels of multibudded cells, compared with mitochore mutants (Figures 1I and 1J). Thus, the multibudded phenotype observed in *mdm10Δ* cells is not a consequence of loss of mtDNA or of defects in mitochondrial respiratory activity, protein import, or OM β-barrel protein assembly. Moreover, we observed a link between the extent of multibudded cells in late-log phase cultures and the severity of the mitochondrial inheritance defect in yeast carrying mutations in mitochore subunits: *mdm10Δ* = *mmm1−1* > > *mdm12Δ* (Figures 1I and 1J). Mdm12p coordinates mitochondrial inheritance and biogenesis through its direct interactions with the PUF family protein Puf3p [11]. Thus, *mdm12Δ* cells may have less severe multibudded and inheritance phenotypes, compared with *mdm10Δ* or *mmm1-1* mutants, because Mdm12p has regulatory effects on mitochondrial motility, whereas Mdm10p and Mmm1p have predominant roles in mediating mitochondrial motility. Overall, the multibudded phenotype observed in all mutants analyzed correlates with defects in mitochondrial inheritance.

*Correspondence: lap5@columbia.edu
[2]These authors contributed equally to this work

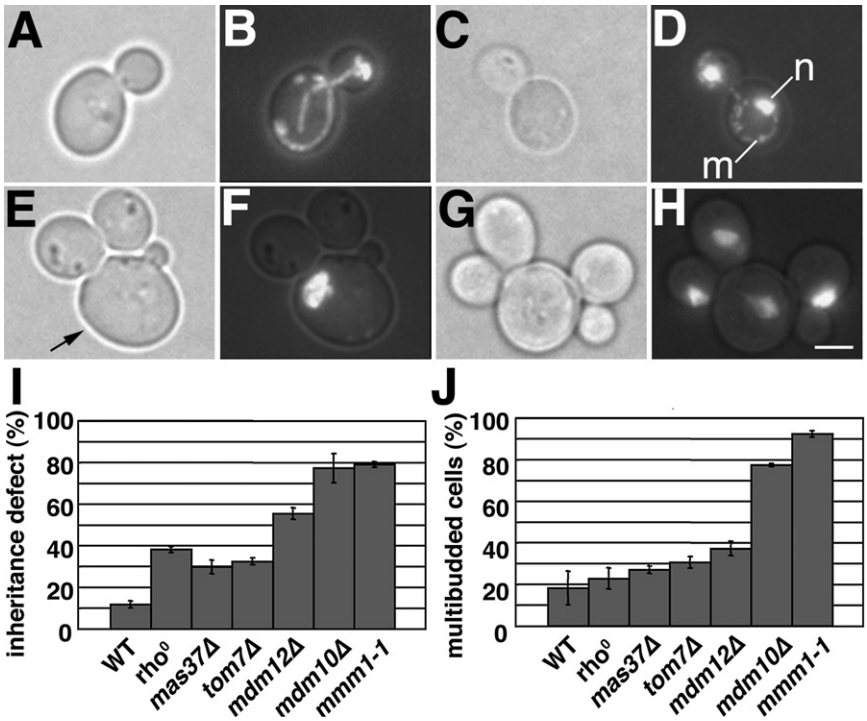

Figure 1. Cell Separation Defects in Mitochondrial Inheritant Mutants

Wild-type (BY4741) or *mdm10Δ* (398) cells were grown in SC medium at 30°C to mid-log phase. Cells were either stained for mitochondria with MitoTracker Red (MtRed) or were fixed with formaldehyde and stained with the DNA-binding dye DAPI. Images of MtRed or DAPI stained cells are 2D projections of the reconstructed 3D volume that are superimposed on the corresponding phase image. The scale bar represents 1 μm.

(A, B, E, and F) Phase images and MtRed staining of wild-type and *mdm10Δ* cells, respectively. The arrow points to the original mother cell in a multibudded *mdm10Δ* cluster that contains a large spherical mitochondrion.

(C, D, G, and H) Phase images and DAPI staining of wild-type and *mdm10Δ* cells, respectively. n denotes nuclear DNA and m denotes mtDNA.

(I and J) Quantification of mitochondria-free buds in cell bearing small buds (I) and multibudded cells (J) in wild-type (ISY001), rho^0 (ISY001-rho^0), *mas37Δ* (ISY005), *tom7Δ* (ISY006), *mdm12Δ* (ISY003), *mmm1-1* (ISY065), and *mdm10Δ* (ISY002) cells (n > 800). Cells were grown in SC medium at 30°C for 12–16 hr to late-log phase (OD_{600} = 1.2–1.4). Error bars are standard deviations (SDs).

mdm10Δ Cells Exhibit Defects in Contractile-Ring Closure

mdm10Δ cells that enter the cell cycle are in G_2 phase 20 min later than wild-type cells (see Figure S1 available online). Spindle assembly and disassembly, as well as the appearance and disappearance of mitotic cyclin, are delayed to a similar extent in *mdm10Δ*, compared with wild-type cells (Figure S2). Formation of the second bud (d2) in multibudded *mdm10Δ* cells occurs 150 min after release from pheromone-induced G_1 arrest, 25 min after the first bud (d1) undergoes Clb2p degradation and spindle disassembly (Figure S2).

rho^0 cells undergo a delay in cell-cycle progression similar to that observed in *mdm10Δ*. The decrease in cell-cycle progression in *mdm10Δ* may be due to loss of mtDNA. However, the multibudded phenotype in *mdm10Δ* cells is not due to loss of mtDNA (Figure 1J) or to defects in septation (degradation of the cell wall between mother and daughter cells), spindle alignment, or nucleolar segregation (Figures S3 and S4). Rather, it is due to defects in contractile-ring closure.

Actomyosin ring contraction was visualized in wild-type and *mdm10Δ* cells by use of a fully functional fusion protein consisting of the type II myosin (Myo1p) fused to GFP [12], mitochondria-targeted DsRed, and 4D imaging (time-lapse imaging combined with 3D reconstruction). Deletion of *MDM10* has no effect on contractile-ring assembly: Myo1p-GFP localizes to a ring at the mother-bud junction in both wild-type and *mdm10Δ* cells (Figures 2A—2D). Moreover, *mdm10Δ* cells have the capacity to undergo contractile-ring closure (Figure 2B), and to do so with kinetics (14.2 ± 3.5 min; n = 48) similar to that of wild-type cells (10.4 ± 2.1 min; n = 43). There is some loss of synchrony in *mdm10Δ* cells at the time of contractile-ring closure. Nonetheless, *mdm10Δ* cells that undergo contractile-ring closure do so 20–40 min later in the cell cycle than do wild-type cells (n = 48).

However, *mdm10Δ* cells exhibit defects in contractile-ring closure, which correlates with defects in mitochondrial inheritance (Figure 2C). To quantitate the frequency of contractile-ring closure, Myo1p-GFP and DsRed-labeled mitochondria were visualized in cells that bore large buds at the onset of imaging for 2 hr. During this time, contractile-ring closure occurred in 100% of the wild-type cells examined (n = 19) and in only 29% of the *mdm10Δ* cell examined (n = 38). To evaluate mitochondrial inheritance as a function of contractile-ring closure, we measured the mitochondrial content in buds of *mdm10Δ* cells that undergo contractile-ring closure (Figure 2B) and in the first buds (d1) of multibudded *mdm10Δ* that failed to undergo contractile-ring closure at the mother cell:d1 junction (Figure 2E). In wild-type and *mdm10Δ* cells that undergo contractile-ring closure, 43% ± 2% (n = 32) and 36.7% ± 3.12% (n = 37) of mitochondria are in the bud, respectively. In contrast, there are no detectable mitochondria in 87% of d1 cells within multibudded *mdm10Δ* cells (n = 100).

Role for the MEN in Regulation of Cell-Cycle Progression in *mdm10Δ* Cells

The MEN regulates cell-cycle progression in response to spindle alignment and elongation and to the transfer of the nucleus from mother to daughter cell during the anaphase-to-telophase transition. Cdc14p activation and localization of the active protein to its sites of action are essential for degradation of a mitotic cyclin (Clb2p), inactivation of a mitotic cyclin-dependent kinase (CDK; Cdc28p/Clb2p), dephosphorylation of CDK substrates, and exit from mitosis [13]. However, several studies indicate that the MEN also plays a direct role in regulating contractile-ring closure during cytokinesis in budding yeast [14–19].

mdm10Δ cells undergoes mitotic exit, as assessed by degradation of Clb2p and spindle disassembly (Figure S2). To evaluate the role of the MEN in the observed cytokinesis defect, we studied the localization of Cdc14p-GFP in *mdm10Δ* and wild-type cells. Cdc14p is released from its inhibitor Cfi1p/Net1p in the nucleolus during two stages in the cell division cycle. In early anaphase, separase, as part

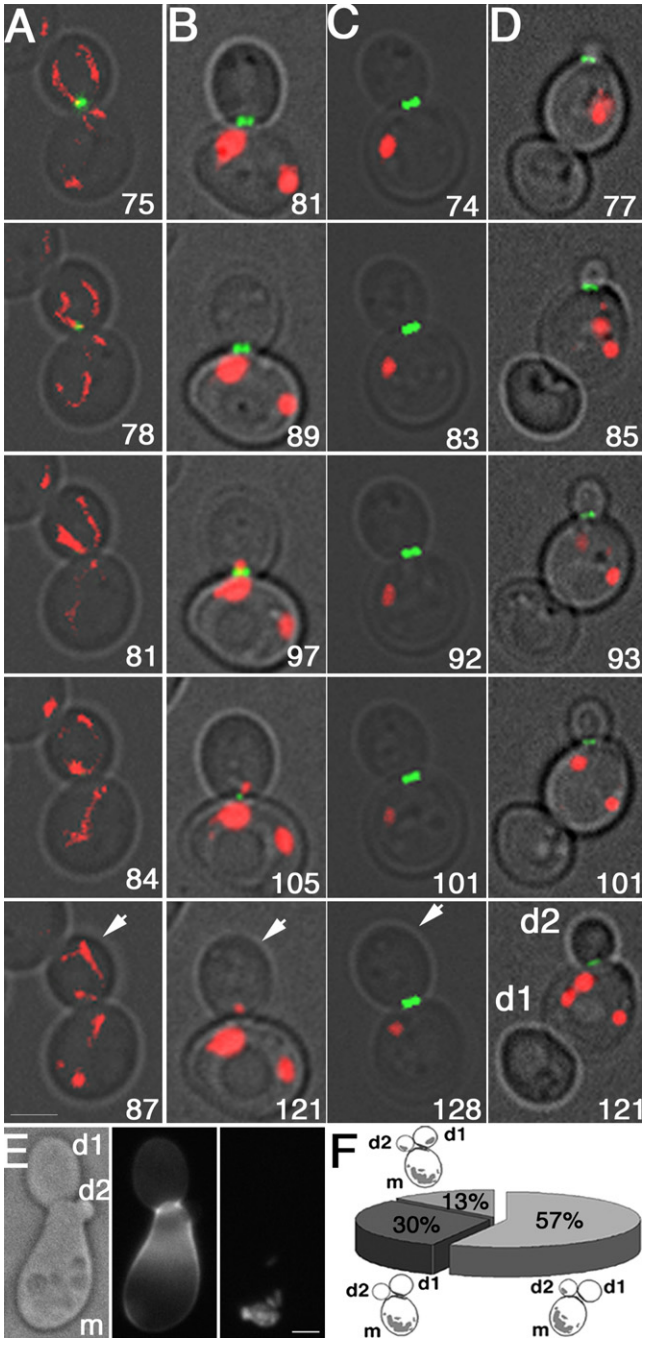

Figure 2. Multibudded Clusters of *mdm10Δ* Cells Are Due to Defects in Contractile-Ring Closure

(A–D) Still frames from time-lapse imaging of Myo1p-GFP (green) and DsRed-labeled mitochondria (red) in synchronized wild-type (ISY008) (A) and *mdm10Δ* (ISY009) (B–D) cells. Unbudded cells were isolated from mid-log phase cultures by centrifugation through a 10%–35% sorbitol gradient for 12 min at 56 × *g* and were visualized by 4D time lapse imaging 1 hr after bud formation, for a total of 1 hr. Images were acquired at 3 and 4 min intervals for wild-type and *mdm10Δ* cells, respectively. Images shown are 2D projections of 3D reconstructions. Arrows point to buds. Numbers indicate time of image acquisition from the onset of bud formation. The scale bar represents 1 μm.

(A) Wild-type cell undergoing contractile-ring closure.

(B) *mdm10Δ* cell that has mitochondria in the bud and undergoes contractile-ring closure.

(C) *mdm10Δ* cell that does not undergo contractile-ring closure and has no detectable mitochondria in the bud.

of the Cdc *f*ourteen *e*arly-*a*naphase *r*elease (FEAR) pathway, promotes a transient and partial release of Cdc14p from the nucleolus. In a second phase, signal transduction through the MEN releases the remaining Cdc14p, which facilitates mitotic exit and cytokinesis [20].

We confirmed that Cdc14p-GFP in wild-type cells localizes to the nucleolus through early stages of the cell division cycle and is released from the nucleolus and localizes to the spindle pole bodies and bud neck as the spindle apparatus elongates (Figure 3A). When the spindle is at its maximum length (6–8 μm), 100% of the Cdc14p-GFP is released from the nucleolus (Figure 3C). In *mdm10Δ* cells, some cytosolic Cdc14p localizes to the spindle pole body in *mdm10Δ* cells bearing fully elongated spindles. However, release of Cdc14p-GFP from the nucleolus is inhibited by 50% in *mdm10Δ* cells bearing 4–6 μm spindles and to a lesser extent in cells with 6–8 μm spindles, compared with wild-type cells (Figures 3B and 3C). Thus, deletion of *MDM10* results in a delay in release of Cdc14p from the nucleolus.

Sli15p, a chromosomal passenger protein and substrate for Cdc14p that is present at kinetochores during metaphase and transfers to the spindle midzone during early anaphase [20], localizes to the spindle to the same extent in *mdm10Δ* and in wild-type cells (Figure S5). Thus, mislocalization of Cdc14p in *mdm10Δ* cells is due to an alteration in MEN-mediated control of Cdc14p and not the FEAR pathway. In light of these findings and our observation that release of Cdc14p from the nucleolus is partially inhibited in *mdm10Δ* cells, it is possible that the level of MEN-mediated Cdc14p activation in *mdm10Δ* cells is sufficient to support mitotic exit but insufficient to support cytokinesis.

Consistent with this, conditions that hyperactivate the MEN promote cytokinesis in *mdm10Δ* cells. Deletion of *BUB2* suppresses the subtle mitotic exit defect observed in *mdm10Δ* cells, but has no effect on the time of entry of *mdm10Δ* cells into anaphase (Figure S6). Deletion of *BUB2* or overexpression of *CDC5* in *mdm10Δ* cells results in a 67% decrease in the number of multibudded cells in late-log phase cell cultures, compared with *mdm10Δ* cells (Figures 4A and 4B). Thus, conditions that bypass MEN regulation bypass the cytokinesis defects observed in *mdm10Δ* cells.

To determine whether other mutations that inhibit mitochondrial inheritance also affect cytokinesis, we studied *GEM1*, a member of the rho (Miro) family of GTPases, and *MMR1*, a protein that localizes to mitochondria in the bud, binds to the type V myosin Myo2p, and is required for anchorage of mitochondria in the bud tip [21, 22]. *mmr1Δ* or *gem1Δ* mutants exhibit subtle defects in mitochondrial inheritance and low but detectable defects in cytokinesis. However, *gem1Δ mmr1Δ*

(D) Multibudded *mdm10Δ* cell in which the first bud (d1) has no detectable mitochondria and a contractile ring has assembled at the site of growth of the second daughter cell (d2).

(E) Mitochondrial morphology and distribution in multibudded cells from synchronized *mdm10Δ* cells. Cells were grown in SC medium at 30°C to mid-log phase (OD_{600} = 0.5–0.8) and were incubated with α-factor (10 μM) for 2.5 hr. Cells were washed and resuspended in medium, fixed at various times after release from pheromone-induced G_1 arrest, and stained with Calcufluor white to stain bud scars on the mother cell (m) but not on the first or second daughter cell (d1 and d2, respectively) produced from that mother cell (middle panel). DsRed-labeled mitochondria are present in the mother cell but not in daughter cells (left panel). The scale bar represents 1 μm.

(F) Quantification of mitochondrial content in mother cells (m) and their first (d1) and second (d2) daughter cells in multibudded *mdm10Δ* cells from synchronized cell cultures. n = 100 clumps with 3 cell bodies.

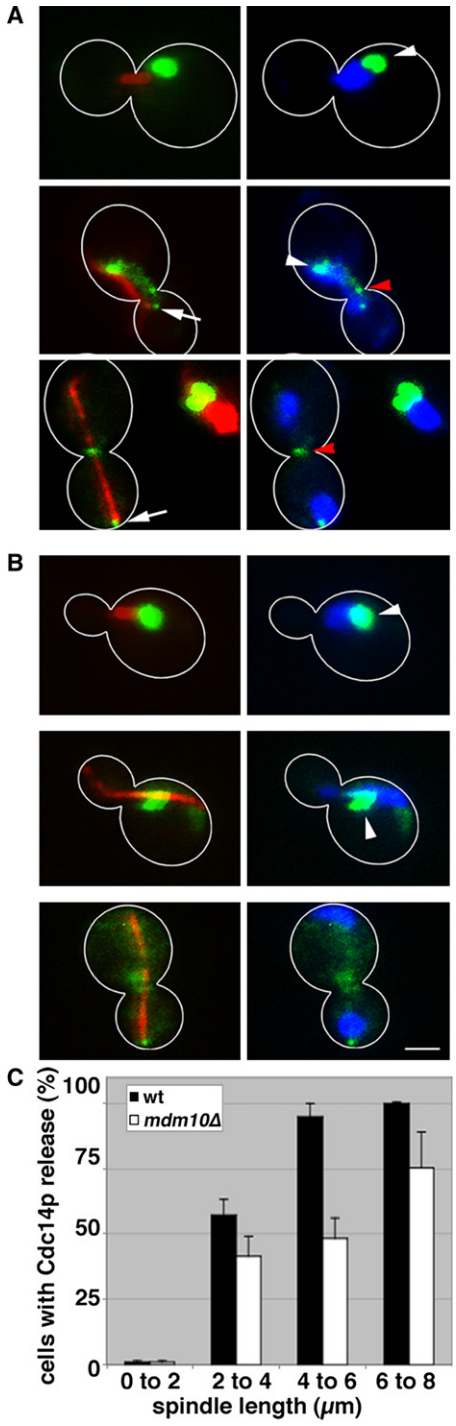

Figure 3. Cdc14p Is Mislocalized in *mdm10⊿* Cells

Wild-type (LGY020) and *mdm10⊿* (LG0Y21) cells expressing Cdc14p-GFP and mCherry-tagged tubulin were grown to mid-log phase, fixed, and stained with DAPI as for Figure 1. The images shown are 2D projections from reconstructed 3D volumes. Overlays of Cdc14p-GFP (green) and tubulin in the mitotic spindle (red) are shown on the left. Overlays of Cdc14p-GFP (green) and DAPI (blue) are shown on the right. Cell outlines are shown in white. White arrow, spindle pole body; white arrowhead, nucleus; red arrowhead, mother-bud neck. The scale bar represents 1 μm.

(A) Cdc14p-GFP localization in wild-type cells. Cdc14p-GFP localizes to the nucleolus in cells bearing short, but detectable spindles (upper panels), to the nucleus and spindle pole bodies in early anaphase when spindles are 4–6 μm in length (middle panels), and to spindle pole bodies and the mother-bud neck during telophase when spindles have elongated and reached their maximum length of 8–10 μm (lower panels).

(B) Defects in localization of Cdc14p-GFP in *mdm10⊿* cells.

(C) Quantitation of the release of Cdc14p from the nucleolus in wild-type and *mdm10⊿* cells as a function of spindle length. Error bars show standard error of the mean (n > 200).

double mutants exhibit mitochondrial distribution and inheritance defects that are significantly greater than those observed in either single mutant [22] and a cytokinesis defect that is more severe than that observed in either single mutants and similar to that observed in the *mdm10⊿* mutant. In addition, deletion of *BUB2* suppresses the cytokinesis defect observed in the *gem1⊿ mmr1⊿* double mutant (Figure 4C). These findings provide additional evidence for the existence of a mechanism to inhibit cell-cycle progression at cytokinesis when there are severe defects in mitochondrial inheritance.

Finally, the primary function of a checkpoint is to ensure that critical cell division processes occur with high fidelity and at the correct time as cells divide. Thus, if the MEN regulates cell-cycle progression in response to mitochondrial inheritance, then hyperactivation of the MEN should reduce the fidelity of mitochondrial inheritance. Indeed, we find that conditions that bypass MEN regulation, deletion of *BUB2* or overexpression of *CDC5*, result in defects in partitioning of mitochondria between mother cells and buds (Figure 4D). Deletion of *BUB2* reduces the amount of mitochondria in daughter cells. Deletion of *MDM10* produces more severe defects in the fidelity of mitochondrial inheritance. Finally, *mdm10⊿* mutants bearing a deletion in *BUB2* or overexpressing *CDC5* exhibit defects in mitochondrial partitioning that are more severe than that in *mdm10⊿* mutants.

Overall, there are numerous cell-cycle checkpoints to monitor events associated with nuclear inheritance, including replication of nuclear DNA and segregation of chromosomes and nuclei. Here, we provide evidence for a mitochondrial inheritance checkpoint that inhibits cytokinesis when there are defects in mitochondrial inheritance in budding yeast, and for a role for the MEN in this process. Because the mitochore has been implicated in association of mitochondria with ER [23], it is possible that these interactions could contribute to cytokinesis. Moreover, in *Drosophila melanogaster*, mitochondrial second messengers, either ROS or ATP, can function as two independent signals to enforce checkpoints at G_1/S that are not due to metabolic restriction [24]. Our findings indicate that a checkpoint for mitochondrial inheritance, which is also independent of metabolic restriction, exists in budding yeast. Finally, because there are mechanisms to ensure the inheritance of many organelles and the MEN is a conserved pathway, our findings also raise the possibility that there are similar checkpoints for organelle inheritance in yeast and other cell types.

Experimental Procedures

Yeast Strains, Plasmids, and Growth Conditions

Yeast strains used in this work are listed in Table S1. *rho*^{0} derivatives were generated from wild-type cells expressing plasmid-borne mitochondria-targeted DsRed (ISY001), as described by Goldring et al. [7]. Other yeast methods were performed according to Sherman [25]. Yeast cell viability was measured with FUN-1 [26].

The carboxy termini of Myo1p and Cdc14p were tagged with GFP via PCR-based insertion into the chromosomal copies of the *MYO1* or *CDC14* loci [27]. Table S2 lists primers used to tag these genes. Standard molecular techniques for cloning procedures were used [28].

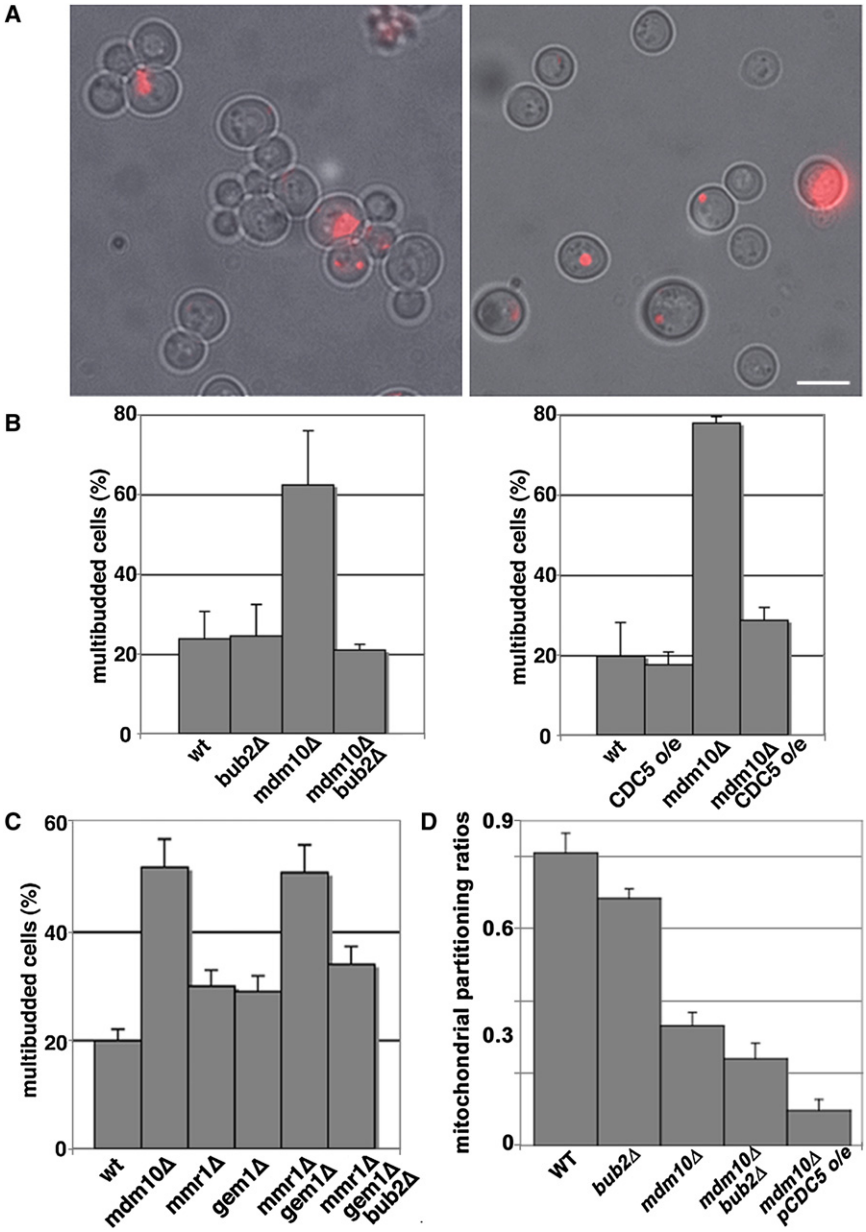

Figure 4. Hyperactivation of the MEN Suppresses the Defect in Cytokinesis Defect Observed in *mdm10Δ* Cells

(A) *mdm10Δ* cells that expressed mitochondria-targeted DsRed and contained either no plasmid (ISY002) or plasmid-borne *CDC5* under control of the GAL promoter (ISY048) were incubated in galactose-based media for 5.5 hr. Images are phase-contrast images superimposed on fluorescence images of DsRed-labeled mitochondria. The scale bar represents 3 μm.

(B) Quantitation of multibudded cells in wild-type cells and *mdm10Δ* cells that overexpress *CDC5* or carry a *BUB2* deletion. Wild-type, *CDC5* overexpression, *mdm10Δ*, and *mdm10Δ* overexpressing *CDC5* strains are ISY001, ISY048, ISY002, and ISY013. Wild-type, *bub2Δ*, *mdm10Δ*, and *bub2Δ mdm10Δ* strains are BY4741, 6189, 398, and LGY025. Cell culture and quantitation were carried out as for Figure 1D. Error bars show SDs (n > 800).

(C) Quantitation of multibudded cells in wild-type (BY4741), *mmr1Δ* (4139), *gem1Δ* (357), *mmr1Δ gem1Δ* (DCY001), and *mmr1Δ gem1Δ bub2Δ* cells (*DCY002*) that were analyzed after treatment with zymolyase 20T (0.1 mg/ml for 10 min at RT). Error bars show SDs (n > 100).

(D) Hyperactivation of the mitotic exit network results in mitochondrial partitioning defects. Mid-log phase wild-type, *bub2Δ*, *mdm10Δ*, *mdm10Δ bub2Δ*, and *CDC5* overexpressing cells (ISY001, ISY028, ISY002, ISY029, and ISY013), which express mitochondria-targeted DsRed, were fixed, and images of yeast bearing large buds (buds ≥ 2/3 the length of their mother cells) were collected at 1-μm z-intervals. Mitochondrial area in the mother cell or bud was measured in each Z section with a user-defined threshold, and these areas were summed over the mother cell or bud to determine mitochondrial volume. Mitochondrial partitioning ratios are the mitochondrial volume in the bud/mother. Error bars show standard error of the mean (n > 250).

Fluorescence Microscopy, Image Analysis, and Cytology

Mitochondria, tubulin, and Sli15p were visualized with plasmid-borne GFP fusion proteins. Chitin in bud scars and DNA were visualized with Calcofluor White and DAPI. Acquisition, manipulation, and analysis of fluorescence images was carried out as described previously [4].

Supplemental Data

Supplemental Data include Supplemental Experimental Procedures, six figures, and two tables and can be found with this article online at http://www.cell.com/current-biology/supplemental/S0960-9822(09)01617-0.

Acknowledgments

We are grateful to A. Amon, J. Shaw, K. Bloom, and E. Schiebel of for plasmids; to J. Aris, A. Amon, T. Davis, D. Kellogg, J. Kitajewski, and G. Schatz for antibodies; to the members of the Pon laboratory for support and critical evaluation; to Jessica Lui for data analysis and interpretation; to K. Gordon in the Flow Cytometry Shared Resource of the Herbert Irving Comprehensive Cancer Center (Columbia University) for assistance with flow cytometry experiments; and to F. Luca and J. Gautier for enlightening discussions. This work was supported by research grants to L.A.P. from the National Institutes of Health (GM45735) and to L.J.G.-R. from the Ramón Areces Foundation (Spain).

Received: October 12, 2008
Revised: July 23, 2009
Accepted: August 13, 2009
Published online: October 8, 2009

References

1. Fehrenbacher, K.L., Yang, H.C., Gay, A.C., Huckaba, T.M., and Pon, L.A. (2004). Live cell imaging of mitochondrial movement along actin cables in budding yeast. Curr. Biol. *14*, 1996–2004.
2. Boldogh, I., Vojtov, N., Karmon, S., and Pon, L.A. (1998). Interaction between mitochondria and the actin cytoskeleton in budding yeast requires two integral mitochondrial outer membrane proteins, Mmm1p and Mdm10p. J. Cell Biol. *141*, 1371–1381.
3. Boldogh, I.R., Nowakowski, D.W., Yang, H.C., Chung, H., Karmon, S., Royes, P., and Pon, L.A. (2003). A protein complex containing Mdm10p, Mdm12p, and Mmm1p links mitochondrial membranes and

DNA to the cytoskeleton-based segregation machinery. Mol. Biol. Cell *14*, 4618–4627.

4. Sogo, L.F., and Yaffe, M.P. (1994). Regulation of mitochondrial morphology and inheritance by Mdm10p, a protein of the mitochondrial outer membrane. J. Cell Biol. *126*, 1361–1373.
5. Hobbs, A.E., Srinivasan, M., McCaffery, J.M., and Jensen, R.E. (2001). Mmm1p, a mitochondrial outer membrane protein, is connected to mitochondrial DNA (mtDNA) nucleoids and required for mtDNA stability. J. Cell Biol. *152*, 401–410.
6. Meisinger, C., Rissler, M., Chacinska, A., Szklarz, L.K., Milenkovic, D., Kozjak, V., Schonfisch, B., Lohaus, C., Meyer, H.E., Yaffe, M.P., et al. (2004). The mitochondrial morphology protein Mdm10 functions in assembly of the preprotein translocase of the outer membrane. Dev. Cell *7*, 61–71.
7. Goldring, E.S., Grossman, L.I., Krupnick, D., Cryer, D.R., and Marmur, J. (1970). The petite mutation in yeast: loss of mitochondrial deoxyribonucleic acid during induction of petites with ethidium bromide. J. Mol. Biol. *52*, 323–335.
8. Wiedemann, N., Kozjak, V., Chacinska, A., Schonfisch, B., Rospert, S., Ryan, M.T., Pfanner, N., and Meisinger, C. (2003). Machinery for protein sorting and assembly in the mitochondrial outer membrane. Nature *424*, 565–571.
9. Honlinger, A., Bomer, U., Alconada, A., Eckerskorn, C., Lottspeich, F., Dietmeier, K., and Pfanner, N. (1996). Tom7 modulates the dynamics of the mitochondrial outer membrane translocase and plays a pathway-related role in protein import. EMBO J. *15*, 2125–2137.
10. Meisinger, C., Wiedmann, N., Rissler, M., Strub, A., Milenkovic, D., Schoenfisch, B., Mueller, H., Kozjak, V., and Pfanner, N. (2006). Mitochondrial protein sorting: Differentiation of β-barrel assembly to Tom7-mediated segregation of Mdm10. J. Biol. Chem. *281*, 22819–22826.
11. García-Rodríguez, L.J., Gay, A.C., and Pon, L.A. (2007). Puf3p, a Pumilio family RNA binding protein, localizes to mitochondria and regulates mitochondrial biogenesis and motility in budding yeast. J. Cell Biol. *176*, 197–207.
12. Lippincott, J., and Li, R. (1998). Dual function of Cyk2, a cdc15/PSTPIP family protein, in regulating actomyosin ring dynamics and septin distribution. J. Cell Biol. *143*, 1947–1960.
13. Stegmeier, F., and Amon, A. (2004). Closing mitosis: the functions of Cdc14 phosphatase and its regulation. Annu. Rev. Genet. *38*, 203–232.
14. Song, S., and Lee, K.S. (2001). A novel function for *Saccharomyces cerevisiae CDC5* in cytokinesis. J. Cell Biol. *152*, 451–469.
15. Luca, F.C., Mody, M., Kurischko, C., Roof, D.M., Giddings, T.H., and Winey, M. (2001). *Saccharomyces cerevisiae* Mob1p is required for cytokinesis and mitotic exit. Mol. Cell. Biol. *21*, 6972–6983.
16. Bembenek, J., Kang, J., Kurischko, C., Li, B., Raab, J.R., Belanger, K.D., Luca, F.C., and Yu, J. (2005). Crm1-mediated nuclear export of Cdc14 is required for completion of cytokinesis in budding yeast. Cell Cycle *4*, 961–971.
17. Blondel, M., Bach, S., Bamps, S., Dobbelaere, J., Wiget, P., Longaretti, C., Barral, Y., Meijer, L., and Peter, M. (2005). Degradation of Hof1 by SCF^{Grr1} is important for actomyosin ring contraction during cytokinesis in yeast. EMBO J. *24*, 1440–1452.
18. Corbett, M., Xiong, Y., Boyne, J.R., Wright, D.J., Munro, E., and Price, C. (2006). IQGAP and mitotic exit network (MEN) proteins are required for cytokinesis and re-polarization of the actin cytoskeleton in the budding yeast, *Saccharomyces cerevisiae*. Eur. J. Cell Biol. *85*, 1201–1215.
19. Clifford, D.M., Wolfe, B.A., Roberts-Galbraith, R.H., McDonald, W.H., Yates, J.R., 3rd, and Gould, K.L. (2008). The Clp1/Cdc14 phosphatase contributes to the robustness of cytokinesis by association with anillin-related Mid1. J. Cell Biol. *181*, 79–88.
20. D'Amours, D., and Amon, A. (2004). At the interface between signaling and executing anaphase-Cdc14 and the FEAR network. Genes Dev. *18*, 2581–2595.
21. Itoh, T., Watabe, A., Toh-E, A., and Matsui, Y. (2002). Complex formation with Ypt11p, a rab-type small GTPase, is essential to facilitate the function of Myo2p, a class V myosin, in mitochondrial distribution in *Saccharomyces cerevisiae*. Mol. Cell. Biol. *22*, 7744–7757.
22. Frederick, R.L., Okamoto, K., and Shaw, J.M. (2008). Multiple pathways influence mitochondrial inheritance in budding yeast. Genetics *178*, 825–837.
23. Kornmann, B., Currie, E., Collins, S.R., Schuldiner, M., Nunnari, J., Weissman, J.S., and Walter, P. (2009). An ER-mitochondria tethering complex revealed by a synthetic biology screen. Science *325*, 477–481.
24. Owusu-Ansah, E., Yavari, A., Mandal, S., and Banerjee, U. (2008). Distinct mitochondrial retrograde signals control the G1-S cell cycle checkpoint. Nat. Genet. *40*, 356–361.
25. Sherman, F. (2002). Getting started with yeast. Methods Enzymol. *350*, 3–41.
26. Millard, P.J., Roth, B.L., Thi, H.P., Yue, S.T., and Haugland, R.P. (1997). Development of the FUN-1 family of fluorescent probes for vacuole labeling and viability testing of yeasts. Appl. Environ. Microbiol. *63*, 2897–2905.
27. Longtine, M.S., McKenzie, A., 3rd, Demarini, D.J., Shah, N.G., Wach, A., Brachat, A., Philippsen, P., and Pringle, J.R. (1998). Additional modules for versatile and economical PCR-based gene deletion and modification in *Saccharomyces cerevisiae*. Yeast *14*, 953–961.
28. Sambrook, J., and Russell, D.W. (1998). Molecular Cloning: A Laboratory Manual, Second Edition (Cold Spring Harbor, NY: Cold Spring Harbor Laboratory Press).